Eurasian Journal of Physics and Functional Materials

Volume 8 | Number 3

Article 1

Pages: 99 - 104

2024

Optimization Of The Photoactive Layer Thickness In Transparent Thin-Film Zno/P3ht:Pcbm Solar Cells

A.K. Abisheva
Buketov Karaganda University, Karaganda, Kazakhstan, a7jan@mail.ru

A.K. Zeinidenov
Buketov Karaganda University, Karaganda, Kazakhstan

A.K. Aimukhanov
Buketov Karaganda University, Karaganda, Kazakhstan

B.R. Ilyassov
Astana IT University, Nur-Sultan, Kazakhstan

Recommended Citation

Abisheva, A.K.; Zeinidenov, A.K.; Aimukhanov, A.K.; and Ilyassov, B.R. (2024) "Optimization Of The Photoactive Layer Thickness In Transparent Thin-Film Zno/P3ht:Pcbm Solar Cells," *Eurasian Journal of Physics and Functional Materials*: Vol. 8: No. 3, Article 1.
DOI: https://doi.org/10.69912/2616-8537.1224

ORIGINAL STUDY

Optimization of the Photoactive Layer Thickness in Transparent Thin-film ZnO/P3HT:PCBM Solar Cells

Assem Abisheva [a,*], Assylbek Zeinidenov [a], Aitbek Aimukhanov [a], Baurzhan Ilyassov [b]

[a] Buketov Karaganda University, Karaganda, Kazakhstan
[b] Astana IT University, Nur-Sultan, Kazakhstan

Abstract

In this article, work was carried out to optimize the thickness of the photoactive layer in inverted solar cells based on ZnO. Fluorine-doped tin oxide (FTO)/ZnO/P3HT:PCBM/MoO_3/Ag organic solar cells were fabricated and characterized. The influence of the thickness of the photoactive layer on the morphology, optical and photoelectric properties of the solar cell has been studied. The surface topography of P3HT:PCBM was examined using atomic force microscopy (AFM). Increasing the thickness of the photoactive layer leads to an increase in the roughness of the film surface. Optical absorption spectra were measured. An increasing trend in absorption was clearly observed when moving from a thinner 85 nm film to a thicker 210 nm film. The P3HT:PCBM film thickness was optimized when deposited at various substrate rotation speeds, with the film produced at 500 rpm achieving a maximum photoconversion efficiency of 1.8%.

Keywords: Spin coating, P3HT:PCBM, Polymer solar cells, ZnO, Inverted organic solar cells, Thickness, Impedance spectroscopy

1. Introduction

Inverted organic solar cells (IOSCs) have recently become very popular among the scientific community due to their low cost, efficiency, environmental friendliness and recyclability [1]. The service life of such solar cells is usually from one hundred to one thousand hours and up to 1 year. Organic solar cells (OSCs) have reached an outstanding certified power conversion efficiency (PCE) of over 19% in single junction, 20% in tandem architecture design and 20.2% (certified 19.8%) in the ternary organic solar cell [2—5]. There are articles in the literature indicating that mixing a polymer with a carbon fullerene in the form of a bulk heterojunction greatly improves the performance of the device. In particular, OSCs based on poly(3-hexylthiophene) (P3HT): phenyl-C61-butyric acid methyl ester (PC61BM) is one of the most popular types. Among the hundreds of material systems available for organic photovoltaic technologies, P3HT:PCBM is the most studied system, the chemical structure of which is shown in Fig. 1a. This is due to the simple synthesis method and the chemical structure of P3HT, which is of interest to chemists for large-scale synthesis. Although P3HT:PCBM blend was introduced into the field of organic photovoltaics more than a decade ago, numerous studies on this polymer blend are ongoing for various applications [6—8].

There are some factors that determine the operating parameters of an organic solar cell. One of them is the thickness of the photoactive layer, which plays an important role in the efficient operation of an organic solar cell due to the shorter exciton diffusion length (<10 nm) and carrier mobility (<10^{-1} $cm^2/V*s$) of polymer materials [9,10]. There are papers in some scientific journals showing that the best device performance and active layer thickness vary depending on the polymers and device configuration [11—13]. In our work, we used a solar cell with the FTO/ZnO/P3HT:PCBM/MoO_3/Ag configuration. The inverted architecture of this solar cell, shown in Fig. 1b, has

Received 10 August 2024; revised 26 August 2024; accepted 3 September 2024.
Available online 19 October 2024

* Corresponding author.
E-mail address: a7jan@mail.ru (A. Abisheva).

https://doi.org/10.69912/2616-8537.1224

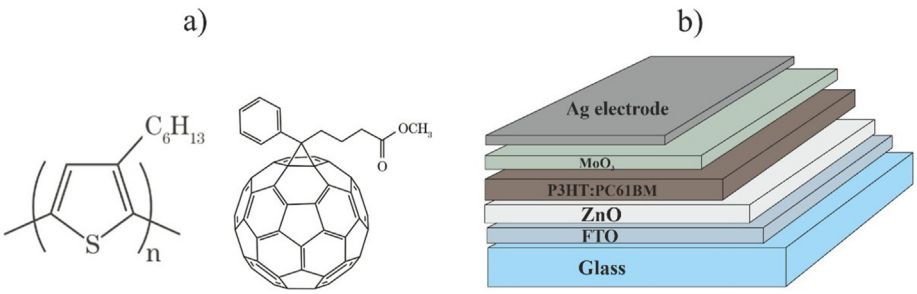

Fig. 1. Chemical structure of PH3T and PCBM and inverted architecture of organic solar cells.

attracted significant research attention due to its stability compared to other organic solar cells.

The efficiency of these inverted solar cells can be further improved by reducing charge recombination and increasing the efficiency of charge transfer between the ETL and the photoactive layer. Therefore, a thin layer of ZnO was deposited on FTO-coated glass substrates to act as an electron transfer layer (ETL). ETL reduces surface recombination by decreasing hole mobility and increasing electron mobility through the layer, resulting in much higher currents, which ultimately increases the fill factor (FF) [14]. A prerequisite for obtaining high efficiency is the optimization of device manufacturing parameters, such as the thickness of the electron transport, hole transport and active layers, annealing after deposition, methods of their deposition, cathode material layer, etc. Since we have already optimized the thickness of the electron transport [15] and hole-transport layers, annealing temperature of the electron transport layer [16] in solar cells of a given configuration, this time we paid attention to optimizing the photoactive layer.

In previous studies, scientists examined the effect of P3HT:PCBM film thickness on the basic characteristics of solar cells. For example [17], presents the complex relationship between film thickness and properties of P3HT:PCBM thin films and shows how different thicknesses affect their structural and optical properties. Thus, they concluded that precise control of film thickness is critical to optimize the performance of organic solar cells. Research team D.W. Zhao in their paper reported the optimization of inverted OSCs by changing the thickness of the photoactive layer and MoO_3 layers with a calcium-based electron transport layer [18]. Shaban, M. and others fabricated the device by changing various parameters including temperature after OSCs production, frequency of active centrifugation layer and the use of Al or Mg-Al as a cathode [19]. Our work is distinctive in that we have fabricated and characterized inverted organic solar cells with the fluorine-doped tin oxide (FTO)/ZnO/P3HT:PCBM/MoO_3/Ag configuration. Many researchers in their works choose TiO_2 as the electron transfer layer, while in this work we used a transparent nanostructured thin film - ZnO. The photoactive layer of the FTO/ZnO/P3HT:PCBM/MoO_3/Ag solar cell was deposited by a simple and economical spin coating method. Among the many film deposition methods, spin coating, despite some limitations, is quite fast, simple, and quite common for producing thin and uniform solution-processed films of active layers for optoelectronic devices [20]. This paper presents the results of a study of the morphological, optical and electrical properties of P3HT:PCBM films, and also studied the effect of their thickness on electronic processes. It should be especially noted that these devices were not encapsulated.

2. Materials and methods

2.1. Sample preparation and deposition process

2.1.1. Solar cell fabrication

Inverted organic solar cells were constructed on glass substrates coated with a thin conductive FTO layer (15 Ω/cm^2) performing the function of an external electrode (cathode). ZnO film was deposited onto the substrate surface using a spin-coater from a solution at a rotation speed of 4000 rpm, followed by annealing at a temperature of 450 °C for 30 min. Next, a photoactive layer was sequentially applied to the ZnO surface. Layers of MoO_3 (Sigma Aldrich, 99.99% purity) and Ag were deposited successively through a shadow mask by thermal evaporation in vacuum at a pressure of 10^{-3} Pa. The films were thermally deposited on a CY-1700x-spc-2 vacuum sputtering unit (Zhengzhou CY Scientific Instruments Co., Ltd). The thickness of MoO_3 and Ag is estimated at 30 nm and 120 nm, respectively. The MoO_3 deposition rate was 0.25 nm/s, and the silver deposition rate was 0.9 nm/s.

2.1.2. Composition of ETL

ZnO solution was prepared by sol-gel method from zinc acetate [Zn $(CH_3COO)_2$ * $2H_2O$] (pure 98%, Sigma Aldrich), isopropyl alcohol (C_3H_8O) (pure 99.9%, Sigma Aldrich) and monoethanolamine (C_2H_7NO)

(MEA, Sigma Aldrich). The resulting solution was stirred on a magnetic stirrer at 60 °C for 2 h. To reduce the oxidation process, all operations were carried out in an airtight glove box.

2.1.3. Organic materials

The photoactive layer was prepared using P3HT:PCBM (Borun New Material Technology). The solution was prepared in a mass ratio of 1:0.9 chlorobenzene. The prepared solution was kept at a temperature of 60° with intensive stirring for 24 h. Application was carried out by spin-coating at 500, 1000, 1500, 2000 rpm/min. The scheme of fabrication an inverted organic solar cells is shown in Fig. 1b.

2.2. Analysis methods

Scanning probe microscopy is used to study the morphology of P3HT:PCBM using an atomic force microscope JSPM-5400 (AFM, JEOL). AFM measurements were conducted using NSG01 (NT-MDT) and NSC14 (Micromash) probes, which have resonant frequencies in the range of 100−200 kHz. Hard tapping mode, characterized by the dominance of repulsive forces, was employed with resonance cantilever amplitude (A_0) of 40−50 nm and a set-point amplitude (A_{sp}) of approximately 0.5A_0 for topography and phase detection. The AFM images were processed using a modular program for analyzing data from scanning probe microscopy (Win SPMII Data-Processing Software).

The absorption spectra of the studied samples were recorded on an AvaSpec-ULS2048CL-EVO spectrometer (Avantes). A combined deuterium-halogen light source AvaLight-DHc (Avantes) with an operating range of 200−2500 nm was used as probing radiation.

Solar cell current-voltage characteristics were measured on a Sol3A Class AAA Solar Simulators (Newport) with PVIV-1AI-V Test Station under illumination from a xenon lamp with an output power of 100 mW/cm^2, calibrated with a silicon reference solar cell (Newport). The impedance spectra were measured on a P45X potentiostat-galvanostat in the impedance mode with an additionally installed FRA-24 M frequency analyzer module. The error in determining the parameters of charge carrier transport did not exceed 5% and was predominantly 1−1.5%. Fitting and analysis of the spectral parameters was performed using the EIS-analyzer software according to the procedure described in [21].

3. Results and discussion

Fig. 2 shows surface images of P3HT:PCBM films deposited on glass substrates at different spin speeds. The surface roughness (Ra) of P3HT:PCBM films was assessed using atomic force microscope (AFM) data. The film deposited at 2000 rpm has a surface roughness of about 1.76 nm. The film deposited at 1500 rpm showed higher roughness compared to the previous film. A further decrease in the centrifugation speed to 1000 rpm led to the production of a film with an even greater surface roughness, reaching a value of 2.49 nm. The film roughness obtained at 500 rpm increased sharply to 6.12 nm and showed the maximum value among the other samples. The dependence of surface roughness on centrifugation speed is presented in Table 1.

The film thickness was measured by AFM. Thickness was assessed by the depth of scratches intentionally applied to the P3HT:PCBM films. As expected, as the centrifugation speed increases, the film thickness becomes thinner. According to AFM data, at 500, 1000, 1500 and 2000 rpm the P3HT:PCBM films have a thickness of about 210, 170, 110 and 85 nm, respectively.

The performance of OSCs has been proven to be enhanced by improving optical absorption [22]. To improve the light absorption of the solar cell, an experiment was carried out to measure the absorption spectra of films at different thicknesses of the photoactive material. The optical absorption spectra shown in Fig. 3a were measured. The absorption of the films increased significantly with increasing thickness. A trend towards increasing absorption is clearly visible when moving from a thinner film with a thickness of 85 nm (black) to a thicker film with a thickness of 210 nm (blue). The findings also indicate efficient absorption of photons by increasing the number density and hence the generation of charge carriers. Based on the picture, the active layer performs well in the near-UV and visible light region, especially from 300 to 650 nm. The absorption shoulder around ~330 nm is due to PCBM, and the main peak at higher wavelengths is due to the absorption of P3HT [23]. The peak at ~490 nm is attributed to interband transitions derived from π−π* transitions between the allowed highest occupied molecular orbital (HOMO) and lowest unoccupied molecular orbital (LUMO) of P3HT:PC61BM. The well-ordered structure of the polymer molecule is indicated by peaks at 600 nm, which were observed in all samples [24]. Fig. 3b shows the Tauc plots from which the band gap (Eg) of P3HT:PCBM was estimated. Table 1 shows the calculated band gaps of films of different thicknesses. This indicates that decreasing the thickness leads to an expansion of Eg from 1.94 eV to 2.14 eV.

Fig. 4 shows the current-voltage characteristics of devices with different active layer thicknesses. As can be seen from the figure, the current-voltage characteristics and cell efficiency depend on the thickness of

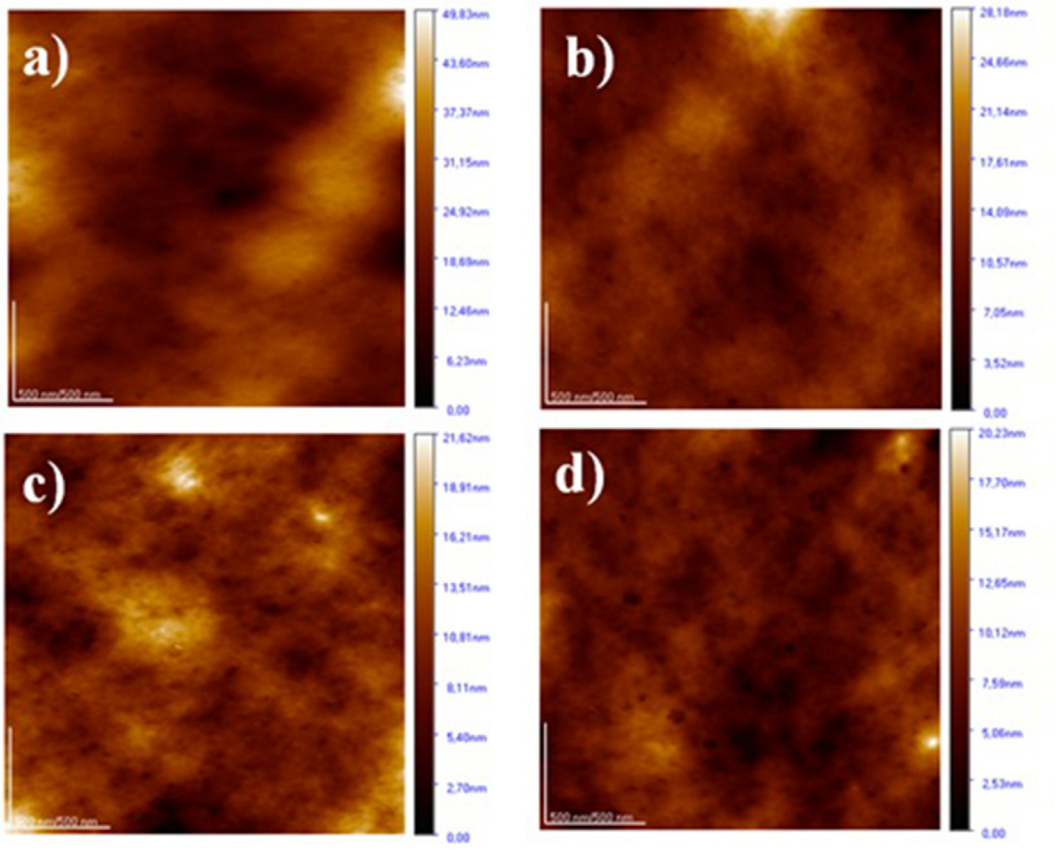

Fig. 2. AFM images of the surface of photoactive layers with different thicknesses: a) 210 nm, b) 170 nm, c) 110 nm, d) 85 nm.

Table 1. The data characterizing the P3HT:PCBM films morphology.

Spin-coating rate, rpm	Thickness, nm	Band gap, eV	Roughness, nm
500	210	1.94	6.12
1000	170	2.14	2.49
1500	110	1.97	2.22
2000	85	2.01	1.76

the photoactive layer. The efficiency of IOSCs at 85 nm thickness is only 0.9%. However, when the thickness of P3HT:PCBM films increases to 210 nm, the efficiency doubles, reaching a value of 1.8%. The short circuit current density (Jsc) varied from 4.3 mA/cm^2 to 7.9 mA/cm^2, which correspondingly affected the cell efficiency. The fill factor (FF) range varied from 37% to 39%. The thickness of the photoactive layer did not have much effect on Voc. The Voc value was approximately 550–610 mV. But J_{sc} changes sharply with thickness and has a maximum value just like FF, which determines the quality of the device in the thickness range of 210 nm. Consequently, the best efficiency was demonstrated by devices with an active layer thickness of 210 nm. Device parameters were low for devices with a smaller active layer thickness, since this thickness might not be sufficient to sufficiently absorb photons incident on the sample. As thickness increases, photon absorption increases, resulting in an increase in short-circuit current density. The obtained device parameters, such as short-circuit current density, duty cycle, open circuit voltage and power conversion efficiency are shown in Table 2.

Fig. 5 presents the impedance spectra (IS) of organic solar cells (OSCs) with varying ZnO electron transport layer (ETL) thicknesses. The IS reveals a single semicircle, indicating that there is predominantly one type of interfacial process occurring within the device. The IS data can be accurately fitted using the equivalent circuit model shown insert to Fig. 5, which consists of a series resistance (R_s) in series with a parallel combination of resistance (R_i) and a constant phase element (CPE). The series resistance (R_s) represents the combined resistances of the electrodes and the active layer, while R_i is associated with charge transfer processes at the interface.

The interpretation of R_i remains a topic of debate in photovoltaic literature. Some researchers define R_i as the charge transfer resistance, while others consider it to be the recombination resistance. In this model, a CPE is used instead of a capacitor to account for the inhomogeneity at the interface.

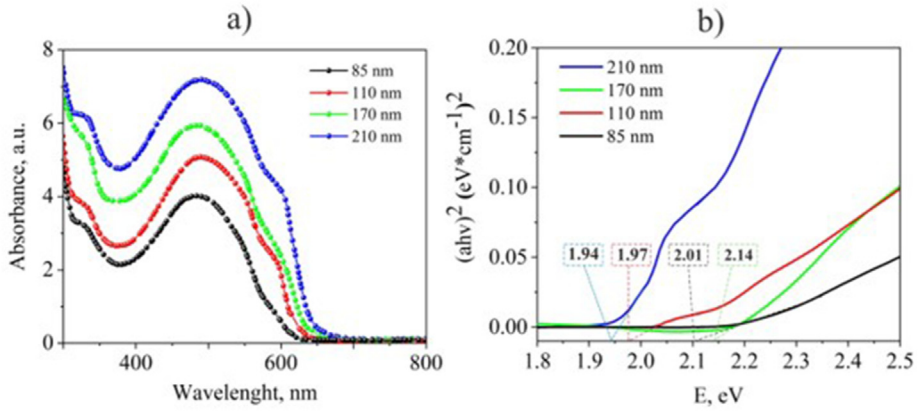

Fig. 3. Absorbance spectra (a) and Tauc plots (b) of the P3HT:PCBM blend with different thicknesses.

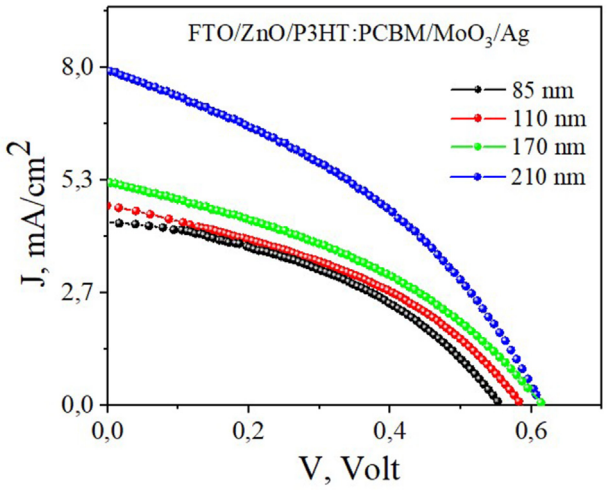

Fig. 4. J-V characteristic curves of the fabricated devices with different thicknesses.

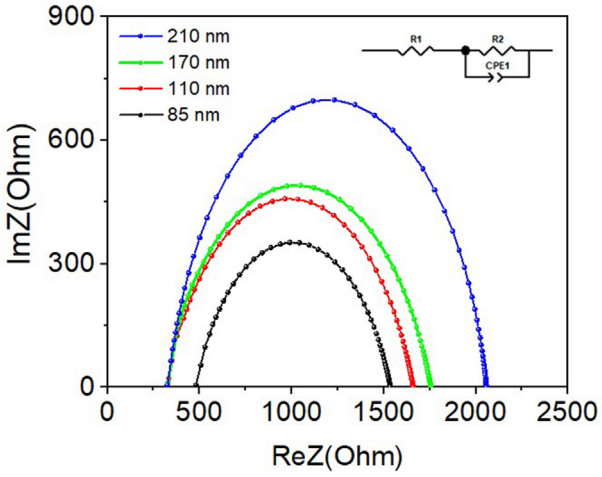

Fig. 5. Impedance spectra and equivalent circuit of devices.

Table 2. Summary of OPVs parameters, Jsc, Voc, FF, and PCE, of devices with different thicknesses.

	I_{sc} mA	V_{oc} V	V_{max} V	I_{max} mA	J_{sc} mA/cm^2	*FF* %	*PCE* %
85 nm	0.69	0.55	0.35	0.41	4.3	38	0.9
110 nm	0.75	0.59	0.37	0.46	4.7	38	1.1
170 nm	0.85	0.61	0.38	0.51	5.3	37	1.2
210 nm	1.27	0.61	0.39	0.78	7.9	39	1.8

Table 3. Equivalent circuit parameters.

Thickness, nm	R_S, (Ohm)	R_{CT}, (Ohm)	CPE-T, (F)	CPE-P
85	480	1057	4.13×10^{-7}	0.75
110	321	1340	2.79×10^{-7}	0.76
170	300	1457	2.95×10^{-7}	0.75
210	330	1729	2.79×10^{-7}	0.76

The impedance spectra were fitted to the equivalent circuit model, with experimental data shown as dots and the fitted data as solid lines. Table 3 lists the equivalent circuit parameters obtained from the fitting. As indicated in Table 3, the device with an 85 nm thick ZnO ETL exhibits the highest R_s, while devices with thicker ZnO ETLs show lower and relatively similar R_s values. The resistance R_i, which we attribute to the recombination resistance, increases with the thickness of the ZnO ETL. This increase is likely due to the reduced areas of direct contact between the active layer and the fluorine-doped tin oxide (FTO) electrode.

4. Conclusion

In this study, we fabricated inverted organic solar cells with FTO/ZnO/P3HT:PCBM/MoO_3/Ag architecture. The effect of the thickness of the P3HT:PCBM photoactive layer on the photovoltaic performance of polymer solar cells was studied. P3HT:PCBM films were deposited from a film-forming solution by spin

coating. The thickness of the photoactive layer was determined from AFM images. As a result of a topography study, it was established that the film obtained by rotating the substrate at a speed of 500 rpm showed the maximum roughness value. The absorption spectra of P3HT:PCBM films were measured. It has been shown that the absorption of films increases with increasing thickness. Measurements of the photoelectric properties of the device with different thicknesses of the photoactive layer showed that the parameters of the current-voltage characteristics depend on the thickness of the P3HT:PCBM films. It was found that the best efficiency was demonstrated for devices with a photoactive layer thickness of 210 nm.

Conflict of interest

The authors have no conflicts of interest to declare that are relevant to the content of this article.

Funding

This research is funded by the Science Committee of the Ministry of Science and Higher Education of the Republic of Kazakhstan (Grant No. AP19679109).

References

[1] F.C. Krebs, et al., Adv. Mater. 26 (1) (2014) 29—38.
[2] S. Rasool, et al., Mater. Futures 2 (2023) 032102.
[3] R. Suthar, et al., Energy Technol. 11 (2023) 2201176.
[4] R. Suthar, et al., J. Mater. Chem. C 37 (2023) 12486—12510.
[5] Y. Jiang, et al., Nat. Energy 9 (2024) 975—986.
[6] L. Liiro-Peluso, et al., ACS Appl. Nano Mater. 5 (2022) 13794—13804.
[7] G. Grancharov, et al., Molecules 26 (2021) 6890.
[8] S.A. Hashemi, et al., Energy Environ. Sci. 13 (2020) 685—742.
[9] O. Inganas, et al., Organic Photovoltaics. Springer Mater. Sci. 60 (2003) 249.
[10] G.H. Bauer, et al., Organic Photovoltaics. Springer Mater. Sci. 60 (2003) 118—158.
[11] X. Zhang, et al., Sol. Energy 147 (2017) 106.
[12] C.J. Brabec, et al., Synth. Met. 121 (2001) 1517.
[13] A.J. Moule, et al., J. Appl. Phys. 100 (1) (2006) 094503.
[14] R.M.G. Wanigasekara, et al., Sri Lankan J. Phys. 22 (2021) 40—49.
[15] T.E. Seisembekova, et al., Appl. Phys. A 128 (2022) 407.
[16] A.K. Abisheva, et al., Eurasian Phys. Tech. J. 18 (2) (2021) 36.
[17] E.E. Igbokwe, et al., J. Chem. Soc. Nigeria 48 (6) (2023) 1051—1066.
[18] D.W. Zhao, et al., Sol. Energy Mater. Sol. Cells 94 (2010) 985—991.
[19] M. Shaban, et al., Coatings 11 (2021) 863.
[20] A.C. Mendhe, Simple Chemical Methods for Thin Film Deposition, 2023, pp. 387—424.
[21] J. Bisquert, et al., Chemelectrochem 1 (1) (2014) 289—296.
[22] P.J. Brown, et al., Phys. Rev. B 67 (2003) 064203.
[23] R. Ramani, et al., Polymer 54 (25) (2013) 6785—6792.
[24] B. Kadem, et al., J. Mater. Sci. Mater. Electron. 27 (2016) 7038—7048.